Geoderma 429 (2023) 116235

Contents lists available at ScienceDirect

Geoderma

journal homepage: www.elsevier.com/locate/geoderma

Plant community mediated methane uptake in response to increasing nitrogen addition level in a saline-alkaline grassland by rhizospheric effects

Xiaopeng Chen [a,b,c], Huajie Diao [a,b,c], Shiping Wang [d], Haiyan Li [e], Zhiping Wang [f], Yan Shen [a,b,c], A. Allan Degen [g], Kuanhu Dong [a,b,c], Changhui Wang [a,b,c,f,*]

[a] College of Grassland Science, Shanxi Agricultural University, Taigu 030801, China
[b] Youyu Loess Plateau Grassland Ecosystem National Research Station, Shanxi Agricultural University, Taigu 030801, China
[c] Shanxi Key Laboratory of Grassland Ecological Protection and Native Grass Germplasm Innovation, Taigu 030801, China
[d] Institute of Tibetan Plateau Research, Chinese Academy of Science, Beijing 100101, China
[e] Key Laboratory of Vegetation Ecology, Ministry of Education, Institute of Grassland Science, Northeast Normal University, Changchun, Jilin 130024, China
[f] Institute of Botany, Chinese Academy of Science, Beijing 100093, China
[g] Desert Animal Adaptations and Husbandry, Wyler Department of Dryland Agriculture, Blaustein Institutes for Desert Research, Ben-Gurion University of the Negev, Beer Sheva 8410500, Israel

ARTICLE INFO

Handling Editor: Jan Willem Van Groenigen

Keywords:
Methane uptake
Nitrogen addition
Plant–microbe interaction
pmoA gene
Salinization

ABSTRACT

Methane (CH_4) uptake in dryland ecosystems is a pathway in mitigating atmospheric CH_4 concentrations. A number of studies have demonstrated that nitrogen availability is a key regulator of the CH_4 oxidation process. However, how plants mediate soil CH_4 oxidation in response to N addition, particularly in saline-alkaline grasslands in the vast regions of the northern China, has received little attention. We conducted a 3-yr (2017–2019) *in-situ* experiment with eight N addition levels to examine the effect of N on soil CH_4 oxidation, and to explore the linkages between the *N*-induced changes of plant community and the seasonal dynamics of CH_4 in a saline-alkaline grassland.

We found that the saline-alkaline grassland was a weak CH_4 sink displaying nonlinear CH_4 uptake levels in response to N additions, possibly due to the nonlinear changes in the abundance of key functional genes (*pmoA*) that were responsible for CH_4 oxidation. The changes in plant productivity and diversity that were induced by N additions explained 21 % of the variations in CH_4 uptake. The *N*-induced increase in productivity indirectly enhanced CH_4 uptake at N addition rates of <10 g m^{-2} yr^{-1}, while the decrease in biodiversity indirectly inhibited CH_4 uptake when N addition exceeded 10 g m^{-2} yr^{-1}. The *N*-induced changes in the plant community can affect CH_4 uptake, mainly through the rhizospheric effects of plants. In conclusion, our findings underscore the importance of rhizosphere when assessing the CH_4 uptake in saline-alkaline grassland ecosystems.

1. Introduction

Biological methane (CH_4) oxidation is the second largest sink after atmospheric photochemical reactions in the troposphere, and dry soils absorb 30 (11–49) Tg CH_4 yr^{-1} (Tian et al., 2016) due to the presence of methanotrophic bacteria, which consume methane as an energy source. Studies have demonstrated that the soil nitrogen (N) availability is an important factor that regulates CH_4 oxidation in soil profiles (Bodelier and Laanbroek, 2004, Aronson and Helliker, 2010, Peng et al., 2019, Chang et al., 2021) and have revealed the mechanisms of CH_4 uptake as a function of N level (Fig. 1). Low levels of N addition stimulate CH_4 uptake in soils (Ma et al., 2020) by increasing methanotrophic growth and enzyme synthesis, whereas high N levels decrease CH_4 uptake due to competition between NH_4^+ and CH_4 for methane monooxygenase (MMO) and the toxic effect of NH_4^+ on methanotrophs (Peng et al., 2019). Most of these studies were performed on acidic and near neutral soils. However, the total area of understudied saline-alkaline soils account for 10 % of the global land area and covers approximately 1.17×10^7 km^2 (Hassani et al., 2020); consequently, an understanding of how N levels affect CH_4 uptake in saline-alkaline soils is crucial to the atmospheric CH_4 budget.

Salinity can affect methane oxidation in several ways (Fig. S1). Setia et al. (2011) reported that exchangeable Na^+ replaced Ca^{2+} and Mg^{2+} to produce soil poor aggregates and increased the dispersion of clay

* Corresponding author at: College of Grassland Science, Shanxi Agricultural University, Taigu 030801, China.
E-mail address: changhui.wang@sxau.edu.cn (C. Wang).

https://doi.org/10.1016/j.geoderma.2022.116235
Received 27 May 2022; Received in revised form 31 July 2022; Accepted 19 October 2022
Available online 31 October 2022

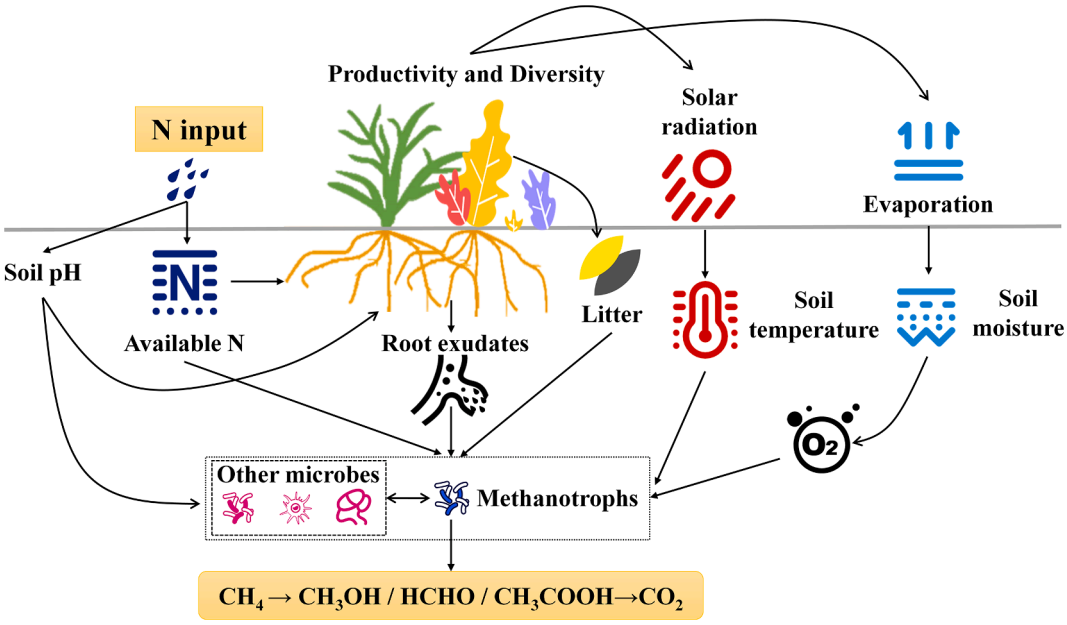

Fig. 1. Schematic representation of the influence mechanism of N enrichment indirectly affecting CH_4 oxidation by changes in plant community.

particles in alkaline soils, which thereby increased the oxygen availability and the level of CH_4 oxidation in soils. High salinities decreased soil CH_4 oxidation due to increases in cell osmotic stress and ion toxicity (primarily Na^+ and Cl^-), decreased the metabolic activity of methanotrophs (Yan and Marschner, 2013) and enzyme activity (e.g., MMO) (Pathak and Rao, 1998) and altered the community composition of methanotrophs (Deng et al., 2017). High pH levels (e.g., 7.5 to 10) reduced MMO activity (Chen et al., 2013), while pH values across cell membranes affected the cell membrane potential differences (Burckhardt et al., 1992) and affected many reactions and the substrate transport of methanotrophs. However, how the *N*-induced changes in soil salinity and pH affect soil CH_4 oxidation is still unclear.

High salinity decreases plant growth, root penetration and microbial activity because of the lowered water availability caused by high osmotic potential of soil solutions (Marschner, 1995). Thus, low soil organic matter deposition and decomposition rates result in low available N in saline-alkaline soils (Wang et al., 2014). Long-term and high-intensity N inputs caused soil acidification due to the loss of basic metal ions with nitrate leaching (Tian and Niu, 2015, Chen et al., 2019). Decreased soil pH inhibited methanotroph activities in neutral or acidic soils but promoted these activities in saline-alkaline soils (Täumer et al., 2020). Therefore, the effects of N additions on CH_4 uptake would differ between saline-alkaline and nonsaline-alkaline soils. However, there is a lack of *in situ* research results as supporting evidence.

N additions increase plant coverage and biomass but decrease plant diversity (Kimmel, et al., 2020). *N*-induced changes of plant community also affect the activity of methanotrophs (Zhang et al., 2019) due to changes in soil temperature and moisture (Aalto et al., 2013) and the interactions among plants and soil microorganisms through changes in root exudates (Huang et al., 2014, Chen et al., 2020a, Moreau et al., 2019). However, the activities of methanotrophs should be independent of plant production since they are autotrophic microorganisms, and their survival does not depend on the products of photosynthesis; thus, the majority of studies have been devoted to assessing the impact of soil environmental factors on CH_4 oxidation rates and methanotrophs in nonsaline-alkaline soils. They found that plants did not affect the CH_4 oxidation process (Lafuente et al., 2019, Zhang et al., 2019, Kou et al., 2021). In contrast, some studies have reported that the interactions among plants and microorganisms increased under adverse conditions (Hu et al., 2018, Willams and de Vries, 2019), as plants and microorganisms formed mutual relationship through plant rhizosphere actions to resist adversity, because plants can provide food for microorganisms and microorganisms may mobilize mineral-bound phosphorus for plants through chelation, complexation and solubilization processes (Trivedi et al., 2020, Liu et al., 2020). With N addition, the plant root traits and the quantities and chemical compositions of root exudates are likely to change (Zhalnina et al., 2018), which may affect methanotrophs by changing the soil permeability and allelopathy. Consequently, we hypothesized that the alterations in the plant community that are induced by N additions would mediate the effects of N additions on CH_4 uptake in saline-alkaline soils.

To determine the effects of N levels on CH_4 fluxes and the underlying mechanisms, we designed a field experiment which used a gradient of eight N levels in an inland saline-alkaline grassland in the Loess Plateau of northern China and measured the *in-situ* CH_4 fluxes during three consecutive growing seasons between 2017 and 2019. Our objectives were to determine (i) the relationship between the CH_4 fluxes and added N levels and (ii) whether the changes in the plant community induced by N additions regulated CH_4 uptake in a saline-alkaline grassland.

2. Materials and methods

2.1. Study site

The study site was in a saline-alkaline grassland at the Youyu Loess Plateau Grassland Ecosystem Research Station (E112°19′39.6″, N39°59′48.5″, 1348 m above sea level), Youyu, Shanxi Province, China. The mean annual temperature is 4.6 °C, and the mean annual precipitation is 425 mm (1991–2019). During the study, the mean air temperatures during the growing seasons (e.g., May to October) in 2017, 2018 and 2019 were 15.4 °C, 14.6 °C and 15.2 °C, respectively, and the rainfall was 356, 489 and 269 mm, respectively (Fig. S3). The soil pH in the topsoil layer (0–10 cm) was 9.0–9.8, and the salinity was 1.44–3.90 g kg^{-1}, with Na^+, HCO_3^- and SO_4^{2-} being the main ions (Chen et al., 2020b). Soil bulk density in top soil (0-10cm) was 1.31-1.37 g cm^{-3}, soil moisture was 16.1%-31.2%, and concentration of soil organic carbon, total nitrogen and total phosphorus were 5.43±0.16, 0.80±0.16 and 0.39±0.01 g kg^{-1}, respectively. The soil was sandy clay loam consisting of 19.3% clay, 24.5 gravel and 56.2% silt. The dominant plant species were *Leymus secalinus*, *Puccinellia distans* and *Saussurea amara*. The study

was conducted as part of the Global Change Network (GCN).

2.2. Experimental design

A randomized block design was used with six blocks, each with 8 plots (each 6 m × 9 m). Eight N levels, in the form of NH_4NO_3, were applied randomly in each block: 0 (N_0), 1 (N_1), 2 (N_2), 4 (N_4), 8 (N_8), 16 (N_{16}), 24 (N_{24}) and 32 (N_{32}) g N m^{-2} yr^{-1} (Fig. S2). The N was added in five equal doses during the growing season (e.g., the first week in May to September). The required amount of NH_4NO_3 for each treatment was dissolved in 10 L of water (equivalent to 0.185 mm rainfall) and was evenly applied over the entire plot. The control treatment received 10 L of water without NH_4NO_3.

2.3. CH_4 flux measurement

The CH_4 fluxes were measured during the 2017, 2018 and 2019 growing seasons by using the static chamber and gas chromatograph method (Chen et al., 2017). In April 2017, a stainless-steel base frame (40 cm × 40 cm) with water grooves was installed at 1 m from the edge of each plot. During gas collection, a dark chamber of 40 cm × 40 cm × 40 cm was mounted on the base frame, and water was added to the grooves to seal the connection between the static chamber and base. The chamber was equipped with an electric fan to mix the air in the headspace and was covered with a plastic film to minimize any fluctuations in the internal air temperatures. To calculate the CH_4 flux rates, four air samples at equal time intervals (e.g., 0, 10, 20, and 30 min) were collected every 2 weeks from 8:00 to 10:00 am (UTC/GMT + 8) from each chamber. The air temperatures inside the chamber were continuously recorded with an electric thermometer (JM224; Jinming Corp., Tianjin, China). Each air sample was collected in a 50-ml plastic syringe fitted with a three-way stopcock connected to the chamber via a Teflon tube and was stored in 100-ml plastic bags (Delin Tech, China). The gas samples were analyzed using a gas chromatograph (Agilent GC-7890B; Agilent Co., Santa Clara, CA, USA) within 7 days of collection.

The CH_4 fluxes were calculated as:

$F_i = \rho_i\ (V/A)\ (P/P_o)\ (T_o/T)\ (d_{Ci}/d_t)$.

where F_i is the flux rate, ρ_i is the density under standard conditions, V is the chamber volume, A is the bottom area, P is the air pressure, P_o is the standard air pressure, T is the air temperature, T_o is the standard temperature, and d_{Ci}/d_t is the CH4 accumulation growth rate (Wei et al., 2015).

2.4. Measurement of biotic and abiotic factors

The air temperatures and precipitation amounts were recorded by a weather station (HOBO U30-NRC; Onset Computer Co., Massachusetts, USA), which was located at a distance of 20 m from the study site. During gas collection, the soil temperatures (ST) and soil volumetric water contents were recorded simultaneously with a TDR-300 probe (Spectrum Technologies Inc., Plainfield, IL, USA).

The plant heights and coverages were measured in mid-August 2017, 2018, and 2019. To determine the aboveground biomass (AGB), all of the biomass in a 0.2 m × 1 m quadrat was harvested according to species and was divided into live matter and litter. The aboveground net primary productivity (ANPP) was determined from the harvested living plant materials. To determine the belowground biomass (BGB) levels, two soil cores each from the main distribution soil layers of the root system in 0–10, 10–20 and 20–30 cm were collected from each quadrat where the AGB was collected. An auger with a 10-cm diameter was used, and two samples from each level were combined. Then, 100-mesh nylon bags were used to clean and remove impurities and to obtain the BGB samples. The in-growth core method was employed to determine the below-ground net primary productivity (BNPP) (Gao et al., 2008) in each soil layer. All aboveground and belowground plant samples were dried at 65 °C for 72 h and were then weighed to determine the AGBs, BGBs, ANPPs and BNPPs. The Shannon-Wiener index was used to determine the biodiversity of the plant community (Spellerberg, 2008). The calculation methods are presented in the Supplementary Information.

At the times of plant sampling, five random soil samples were collected from the upper 10-cm of the soil by using a 5-cm diameter auger in each plot, and each sample was mixed by the five soil cores. The samples were combined and passed through a 2-mm mesh to remove plant residues, visible roots, gravels and stones. Each soil sample was separated into four subsamples. The first sample was air dried and transported to the laboratory to measure the soil pH; the second sample was stored at −80 °C for DNA extraction; the third sample was used to determine the NH_4^+-N and NO_3^--N concentrations within 24 h; and the fourth sample was stored at 4 °C for determinations of the dissolved organic N (DON), microbial biomass carbon (MBC) and microbial biomass N (MBN) levels.

The soil pH levels were determined by a pH meter (PHS-3C; INESA Co., Shanghai, China), with a ratio of deionized water to soil of 2.5:1. The ammonium acetate extraction method with an atomic absorption spectrometer (AAS, Shimadzu, Kyoto, Japan) was used to determine the soil cation exchange capacities. The soil bulk densities (BD) were calculated from the dry soil weights contained in 100 cm^3 of intact soil cores. The water-filled pore spaces (WFPS) were calculated by using the soil volumetric water contents and measured bulk densities, with a theoretical particle density of 2.65 g cm^{-3} (Zhang et al., 2014). To extract NH_4^+-N and NO_3^--N, 100 mL of 2 mol/L KCl was added to 25 g of soil and centrifuged at 220 rpm for 30 min, and the NH_4^+-N and NO_3^--N concentrations were measured using a flow injection analyzer (Auto-analyzer 3 SEAL, Norderstedt, Germany). The above extracts were analyzed in a TOC (Total organic carbon) analyzer (Multi N/C 3100; Jena, Germany) to determine the total dissolved N (TDN). The DON was equal to the TDN minus the sum of NH_4^+-N and NO_3^--N. The MBC and MBN were determined as the differences between the dissolved C/N concentrations in 100 mL 0.5 mol/L K_2SO_4 extracts of 25 g soils that were either extracted directly for 30 min or fumigated with $CHCl_3$ for 24 h prior to the 30 min 0.5 M K_2SO_4 extraction and used K_{EC} and K_{EN} factors of 0.45 and 0.50, respectively (Farrell et al., 2014). The extracts obtained from the samples were measured for their MBC contents with the TOC analyzer, while the MBN contents were determined with a flow injection analyzer.

The abundance of the *pmoA* (the key functional gene controlling the synthesis of particle MMO) gene in the soil samples collected in August 2019 was determined by using the primer pair A189f (5′-GGNGACTGGGACTTCTGG-3′)/Mb661r (5′-CCGGMGC- AACGTCYT-TACC-3′) (Kolb et al., 2003). DNA extraction was conducted using a FastDNA Spin kit (Qiagen Co., Hilden, Germany) with 0.25 g of soil. The quality and quantity of the DNA were assessed through gel electrophoresis with a Nanodrop ND-2000 UV–vis Spectrophotometer (Nanodrop Technologies, Wilmington, DE, USA.). Then, the total gDNA was taken for PCR/qPCR determinations, and the 20-μL reaction mixtures were first connected to the T vector (InsTAclone PCR Cloning Kit, K1213, Fermentas Inc.; Burlington, Ontario, Canada) and constructed the standard product and standard curve [y = -3.08 log (x) + 38.98, R^2 = 0.99; the amplification efficiency was 112 %] was constructed. The qPCR system was configured with 10 μl of qPCR Mix (SinoGene, Beijing, China), 0.5 μl of forward/reverse primers (5 μM), 1 μl of DNA, and 8.5 μl of ddH_2O, and the reaction was conducted on a quantitative PCR machine (Mx3000P, Stratagene; Agilent Co., Santa Clara, CA, U.S.A.). The reaction program consisted of predenaturation at 95 °C for 2 min, 40 cycles of 95 °C for 20 s, annealing at 56 °C for 30 s, and extension at 60 °C for 45 s. The gene contents of each sample were determined according to the standard curve.

The rhizosphere and bulk soil fractions were sampled in Mid-August 2020. The volume of 20 × 20 × 20 cm (depth) soils containing the root system were collected (Hu et al., 2018), in each plot where the AGB were harvested in each plot. In order to collect bulk soil, plants were shaken

Table 1
Results (F value) of two-way repeated measures ANOVAs on the effects of nitrogen additions (N), experimental year (Y), and their interactions (N × Y) on biotic and abiotic variables. *, ** and *** denoted $p < 0.05$, $p < 0.01$, $p < 0.001$, respectively.

Variable	N	Y	N × Y
ST (℃)	1.80	1490.85***	0.95
Soil pH	2.23	76.05***	0.77
WFPS (%)	0.22	87.44***	0.72
NH_4^+-N (mg kg^{-1})	13.95***	589.43***	13.44***
NO_3^--N (mg kg^{-1})	143.41***	32.18***	6.73***
DON (mg kg^{-1})	3.28**	11.66***	2.21*
MBC (mg kg^{-1})	1.30	170.22***	1.51
MBN (mg kg^{-1})	0.79	92.23***	1.30
MBC:MBN	2.68*	8.85**	1.22
ANPP (g m^{-2})	3.76**	30.94***	1.89*
AGB (g m^{-2})	2.50*	44.30***	1.04
0–30 cm BNPP (g m^{-2})	1.64	9.54***	0.99
0–30 cm BGB (g m^{-2})	1.75	70.57***	1.74
BGB:AGB ratio	3.36**	90.83***	2.00*
Coverage (%)	1.12	155.41***	3.08**
Shannon-Weiner index	4.07**	191.91***	2.61**

vigorously by hand for 10 min, paying attention to the root's integrity at the same time (Barillot et al., 2013). Rhizosphere soil was afterwards collected by using a small brush to remove the adhering soil of roots. The bulk and rhizosphere soil samples were passed through a 2 mm mesh to remove plant residue and visible roots, then the soil sample were separated into two subsamples. One set of subsamples was air dried then transported to laboratory to determine the soil pH. The second set of subsamples was stored at −80 °C for DNA extraction and to determine the *pmoA* gene abundance (same method as above).

2.5. Statistical analysis

All data are presented as the means ± SE (n = 6), unless otherwise stated. The data were tested for normality and homogeneity of variance before analysis, and only the WFPS results conformed to a normal distribution were selected. The other data did not satisfy the assumptions of normality and were subjected to ANOVA after normal transformations (logarithmic conversions). The effects of N level, year and their interactions were analyzed by two-way repeated-measures ANOVA. The built-in SPSS (SPSS version 22.0, SPSS Inc., Chicago, IL, USA) linear mix model was used for multiple comparisons of the environmental factors, vegetation characteristics, soil properties and CH_4 fluxes between treatments to eliminate the random effects of replication (Tukey, $p < 0.05$) (Bolker et al., 2009). The response ratio (RR) of the soil CH_4 uptake to the level of N was calculated as follows:

$y = ln(x_t/x_c)$where y is the RR and x_t and x_c represent the mean values of the treatment and control, respectively (Hedges et al., 1999). Linear and quadratic functions were used to fit the relationships among biotic/abiotic factors and N levels, and the best fitting models were selected using the Akaike information criterion (AIC) (SPSS version 22.0, SPSS Inc., Chicago, IL, USA). Redundancy analysis (RDA) was applied to evaluate the relationships among the functional traits (*pmoA* gene abundances and CH_4 uptake rates) and environmental factors (biotic and abiotic factors) by using the Vegan package in the R statistical computing platform.

Structural equation models (SEMs) were generated to determine the direct and indirect biotic and abiotic drivers of soil CH_4 uptake, and the theoretical basis of the influence path is shown in Fig. 1. Owing to the collinearity among some variables, we conducted principal component (PC) analysis to create a multivariate functional index before SEM construction. The first component (PC1), which explained >60 % of the total variance for these four groups, was then introduced as a new variable to represent the combined group properties in the subsequent analysis. The best fitting models were selected using the χ^2 test, low root square mean error of approximation (RMSEA), goodness-of-fit index (GFI), comparative fit index (CFI) and AIC (Hooper et al., 2008). The degree of model fit after adding or abandoning the path was evaluated according to the above indices for each path selection or abandonment. The SEMs used Amos version 23.0 (SPSS Inc., Chicago, IL, U.S.A.).

3. Results

3.1. Responses of biotic and abiotic factors to N levels

In 3 years of field experiment, nitrogen addition altered potential influencing factors on methane fluxes. The nitrogen additions increased

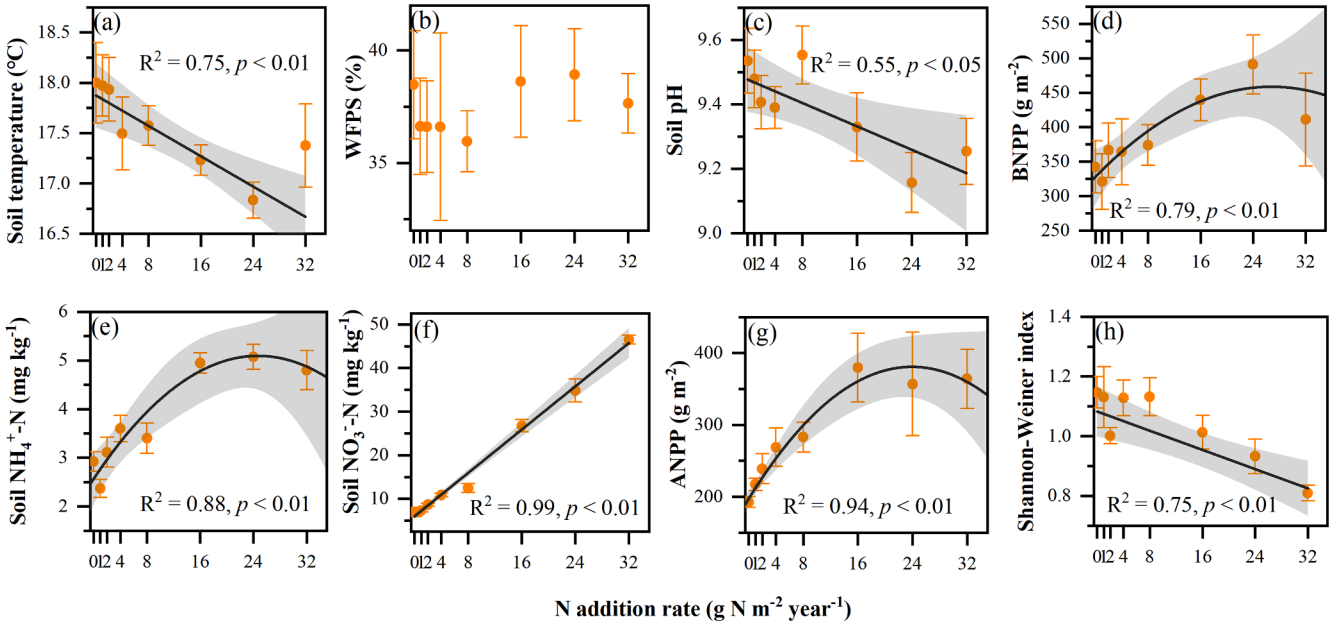

Fig. 2. Changes in soil temperature (a), water fill pore space (WFPS) (b), soil pH (c), BNPP (d), soil NH_4^+-N concentration (d), soil NO_3^--N concentration (e), ANPP (g) and Shannon-Wiener index (h) along the N addition rate, each point was mean of 2017, 2018 and 2019 growing seasons. Solid black lines indicate mean estimates and the shaded areas in gray denote 95 % confidence intervals.

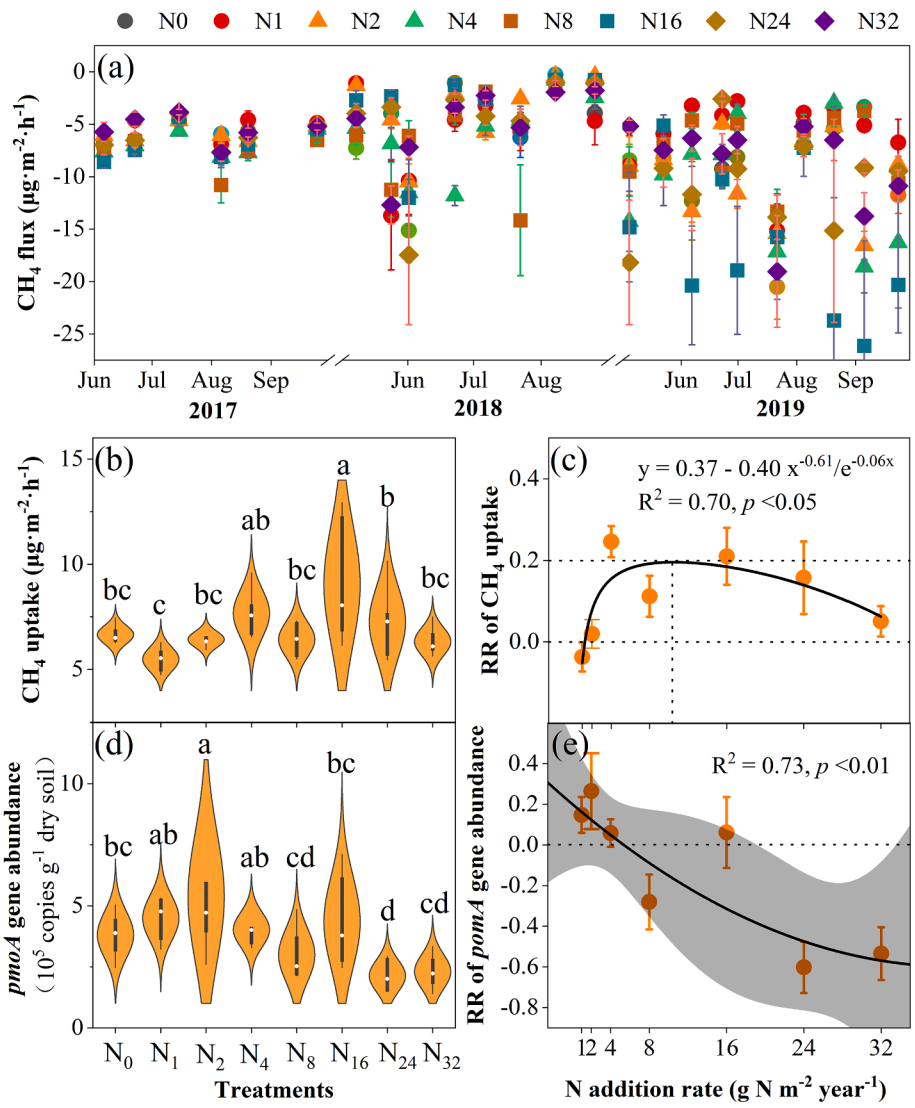

Fig. 3. Seasonal variation of CH_4 flux under eight levels N addition in 2017, 2018 and 2019 growing seasons (a), bars represent the means and standard errors (n = 6). Linear mixed model results of treatment effects on seasonal mean value of CH_4 uptake during 2017–2019 growing seasons (b) and on *pmoA* gene abundance in mid-August 2019 (d), different lowercase letters denoted significant difference between treatments ($p < 0.05$). N0, N1, N2, N4, N8, N16, N24 and N32 represent the N addition rates of 0, 1, 2, 4, 8, 16, 24, and 32 g N m^{-2} $year^{-1}$, respectively. Relationship between the response ratio (RR) of CH_4 uptake (mean of 2017, 2018 and 2019 growing seasons) and N addition rate (c), and relationship between the RR of *pmoA* gene abundance and N addition rate in the mid-August 2019 (e).

the soil NH_4^+-N, NO_3^--N, DON, MBC:MBN, AGB and ANPP ($p < 0.05$) but decreased the BGB:AGB ratio and Shannon–Wiener index ($p < 0.05$) (Table 1). All of the biotic and abiotic factors differed among years ($p < 0.01$), and the N addition affected interannual variation (N level × year interaction) in soil NH_4^+-N, NO_3^--N, DON, ANPP, ANPP:BNPP ratio, plant coverage and Shannon–Wiener index ($p < 0.05$).

The biotic and abiotic factors changed along nitrogen addition levels. The soil temperatures (Fig. 2a) and pH (Fig. 2c) and Shannon–Wiener index (Fig. 2h) decreased by 0.04℃, 0.01 and 0.008, respectively, with each increase of 1 g N m^{-2} yr^{-1} (Table S1). The soil NO_3^--N (Fig. 2f) concentrations increased by 1.24 mg kg^{-1} with each increase of 1 g N m^{-2} yr^{-1} (Table S1). The soil NH_4^+-N (Fig. 2e), ANPP (Fig. 2g), 0–30 cm BNPP (Fig. 2d) and soil exchange capacity of soil Ca^{2+} (Fig. S4c) first increased initially with an increased N addition rate, while they exhibited slight downward trends when the N addition rates were >24 g N m^{-2} yr^{-1}. The N levels had no effects on the WFPS (Fig. 2b) or the exchange capacity of soil Na^+ (Fig. S4a), K^+ (Fig. S4b), or Mg^{2+} (Fig. S4d).

3.2. Responses of CH_4 uptake rates and pmoA gene abundance to N levels

The saline-alkaline grassland was a weak atmospheric CH_4 sink (Fig. 3a). The mean uptake rate was 6.54 ± 0.16 μg $m^{-2}h^{-1}$ in the control (N_0) plots, with a range of 3.30 ± 0.26 to 16.27 ± 3.20 μg $m^{-2}h^{-1}$ in all plots (Fig. 3b). The mean CH_4 uptake rate of N_{16} was significantly higher than those of N_0 (35.0 %), N_1 (60.6 %), N_2 (38.4 %), N_8 (35.6 %), N_{24} (23.3 %), and N_{32} (41.3 %) ($p < 0.05$), while those of N_4 (38.2 %) and N_{24} (30.2 %) were higher than that of N_1, whereas there were no differences among the other treatments ($p > 0.05$) (Fig. 3b). Nitrogen promoted CH_4 uptake in the salinized grassland (CH_4-RR values > 0) (Fig. 3c) and the correlation between CH_4-RR and N additions was best expressed by a peak function (Table S2), where the CH_4-RR peaked at 10.12 g N m^{-2} yr^{-1} (Fig. 3c). The effects of added N amounts on CH_4 uptake and the correlation between CH_4-RR and N additions in each observation year are presented in Fig. S5.

The abundances of *pmoA* gene, which is the key functional gene controlling the methane oxidation process varied from 1.83 ± 0.23 × 10^5 to 4.59 ± 0.92 × 10^5 copies g^{-1} dry soil (Fig. 3d). The *pmoA* gene abundance in N_2 was higher than that in N_0 (42.55 %), N_8 (80.00 %), N_{16} (24.05 %), N_{24} (150.82 %), and N_{32} (132.99 %), and that in N_1 was higher than those in N_8 (49.02 %), N_{24} (107.65 %) and N_{32} (92.89 %); N_4 was higher than those in N_8 (35.69 %), N_{24} (89.07 %) and N_{32} (75.63 %); and N_{16} was higher than that in N24 (102.19 %) ($p < 0.05$). The correlation between *pmoA*-RR and N addition rates was best expressed by a polynomial equation (Table S2). N additions increased the *pmoA* gene abundances (*pmoA*-RR value > 0) when the N addition rates were <6.75 g m^{-2} yr^{-1}, while they decreased the *pmoA* gene abundances (*pmoA*-RR value < 0) when the N addition rates were >6.75 g m^{-2} yr^{-1} (Fig. 3e).

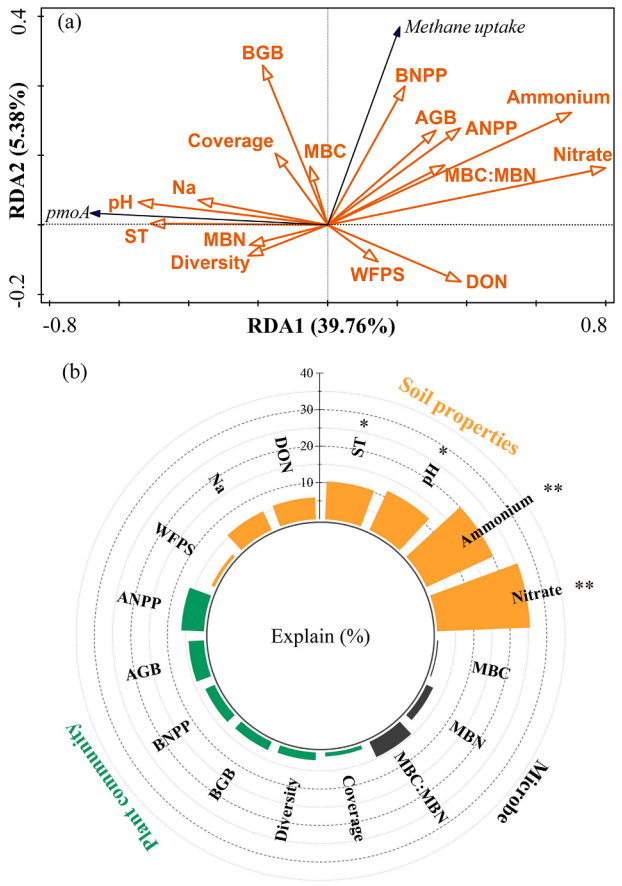

Fig. 4. Redundancy analysis (RDA) showed the *pmoA* gene abundance and CH_4 uptake rate are explained by biotic and abiotic factors (a), and the explains of each factor (b). * and ** denoted $p < 0.05$ and $p < 0.01$, respectively.

3.3. Effects of biotic and abiotic factors on CH_4 uptake

Redundancy analysis (RDA) results revealed that the abiotic and biotic factors explained 39.76 % and 5.38 % of the variations of *pmoA* gene abundance and CH_4 uptake on the first and second axes, respectively (Fig. 4a). The soil NO_3^--N ($R^2 = 0.25$, $p < 0.01$); NH_4^+-N ($R^2 = 0.20$, $p < 0.01$); pH ($R^2 = 0.12$, $p < 0.05$) and soil temperature ($R^2 = 0.10$, $p < 0.05$) were the major drivers of the *pmoA* gene abundances and CH_4 uptake rates (Fig. 4b). However, the effects of abiotic and biotic factors on *pmoA* gene abundances and CH_4 uptake rates were not consistent. The AGB, ANPP, BGB, BNPP, MBC: MBN, NH_4^+-N and NO_3^--N, which have longer projection on the CH_4 uptake arrow have stronger positive correlations with CH_4 uptake, whereas soil temperature, pH, and exchangeable Na^+ have stronger positive correlations with the *pmoA* gene abundances.

According to the relationship between CH_4-RR and N levels (Fig. 3c), we can divide N addition into two scenarios: low nitrogen (<10 g N m^{-2} yr^{-1}) and high nitrogen (>10 g N m^{-2} yr^{-1}) additions. And the structural equation model analyses suggested the biotic and abiotic drivers of CH_4 uptake under all treatments, low and high N additions (Fig. 5). Under all treatments, the nitrogen additions induced changes in root activity, and the soil environmental factors promoted CH_4 uptake, while the changes in microbial biomass C and N decreased the CH_4 uptake levels (Fig. 5a). Although the direct positive effects (path coefficient = 0.27) and indirect negative effects (path coefficient = -0.24) of vegetation on the CH_4 uptake levels nearly offset each other, combined changes of vegetation and roots explained 21 % of the CH_4 uptake changes (Fig. 5b). Under the scenario of low N addition, the *N*-induced changes in the soil pHs and soil NO_3^--N concentrations directly promoted CH_4 uptake, and the plant productivities indirectly promoted CH_4 uptake, while the changes in microbial biomass C and N directly inhibited CH_4 uptake (Fig. 5c). Increased plant productivity levels explained 14 % of the variations in CH_4 uptake (Fig. 5d). Under the scenario of high N addition, decreased pH promoted while the changes in microbial biomass C and N inhibited CH_4 uptake (Fig. 5e). The N addition induced decreased plant biodiversity indirectly inhibited CH_4 uptake (Fig. 5e) and explained 16 % of the variations in CH_4 uptake (Fig. 5f).

3.4. N-induced rhizospheric effects on pmoA gene abundance

To ascertain the influences of plant community characteristics on soil CH_4 oxidation, we further analyzed the rhizospheric effect on soil pH, inorganic N concentration and *pmoA* gene abundance. The result showed that soil pH in the rhizosphere soils were approximately 0.6 units lower than that in the bulk soils, and the soil pH of rhizosphere soils decreases faster (2 times, the slopes were −0.02 vs −0.01) than bulk soils with the increasing N addition (Fig. 6a). While the inorganic N concentration in rhizosphere soils were higher than bulk soils and the inorganic N concentration in rhizosphere soils increases faster (4 times, the slopes were 2.86 vs 0.67) than bulk soils with the increasing N addition (Fig. 6b).

Rhizospheric effects of salinized grassland on soil pH and inorganic N concentration then affect the response of *pmoA* gene abundance to N addition. According to the relationship between *pmoA*-RR and N levels (Fig. 3e), we divided N addition into low and high N additions with the critical value was 7 g N m^{-2} yr^{-1}. High N addition decreased *pmoA* gene abundance in rhizosphere and bulk soils by 51 % and 61 %, respectively (Fig. 6c). Rhizospheric effects significantly increased *pmoA* gene abundance under low N addition by 54 %, while had no impact under high N addition.

4. Discussion

4.1. Low CH_4 uptake rates in saline-alkaline soil

The CH_4 uptake level for the saline-alkaline grassland, 6.54 μg $m^{-2}h^{-1}$, was lower than that of nonsaline grassland (soil pHs ranged from 7.1 to 7.6), which ranged between 20.8 and 71.5 μg $m^{-2}h^{-1}$ for a typical steppe (Li et al., 2018), shortgrass steppe (Mosier et al., 2003), alpine steppe (Wei et al., 2014) and montane grassland (Unteregelsbacher et al., 2013). The CH_4 uptake of the saline-alkaline grassland was comparable to the values determined under some extreme climatic conditions or for soils with severe acidification. For example, the CH_4 uptake rate was only 10.5 μg $m^{-2}h^{-1}$ in a temperate desert with limited precipitation (216 mm) (Yue et al., 2019), 12.1 μg $m^{-2}h^{-1}$ in an alpine meadow with low air temperatures (-5.2°C) (Chen et al., 2017), and ~5.45 μg $m^{-2}h^{-1}$ in a forest plantation with a soil pH of 4.3 (Li et al., 2015). The *pmoA* gene abundance (copies g^{-1} dry soil) in saline-alkaline soil was 3.22×10^5, which was lower than the range between 9.0×10^5 and 2.2×10^7 determined for tropical forest soils with pHs from 5.21 to 7.53 (Bhardwaj and Dubey, 2020) and was considerably lower than the range between 2×10^7 and 12×10^7 that was determined for an alpine steppe with a pH of 8.46 (Peng et al., 2019). Thus, the key functional gene abundances explain the low CH_4 uptake rates in the saline-alkaline grassland: salinization inhibits the activity of methanotrophs.

4.2. Mechanisms of unimodal CH_4 uptake in response to increasing N levels

Methanotrophs use CH_4 as both an energy and carbon source and absorb N from the soil (Bürgmann, 2011). The RRs of the *pmoA* gene abundance were >0 with low N additions and were <0 with high N additions, which explained the unimodal pattern of soil CH_4 uptake in response to increasing N levels. However, the N threshold for the RR of CH_4 uptake was 10.12 g N m^{-2} yr^{-1} (Fig. 2c) and that for RR of *pmoA*

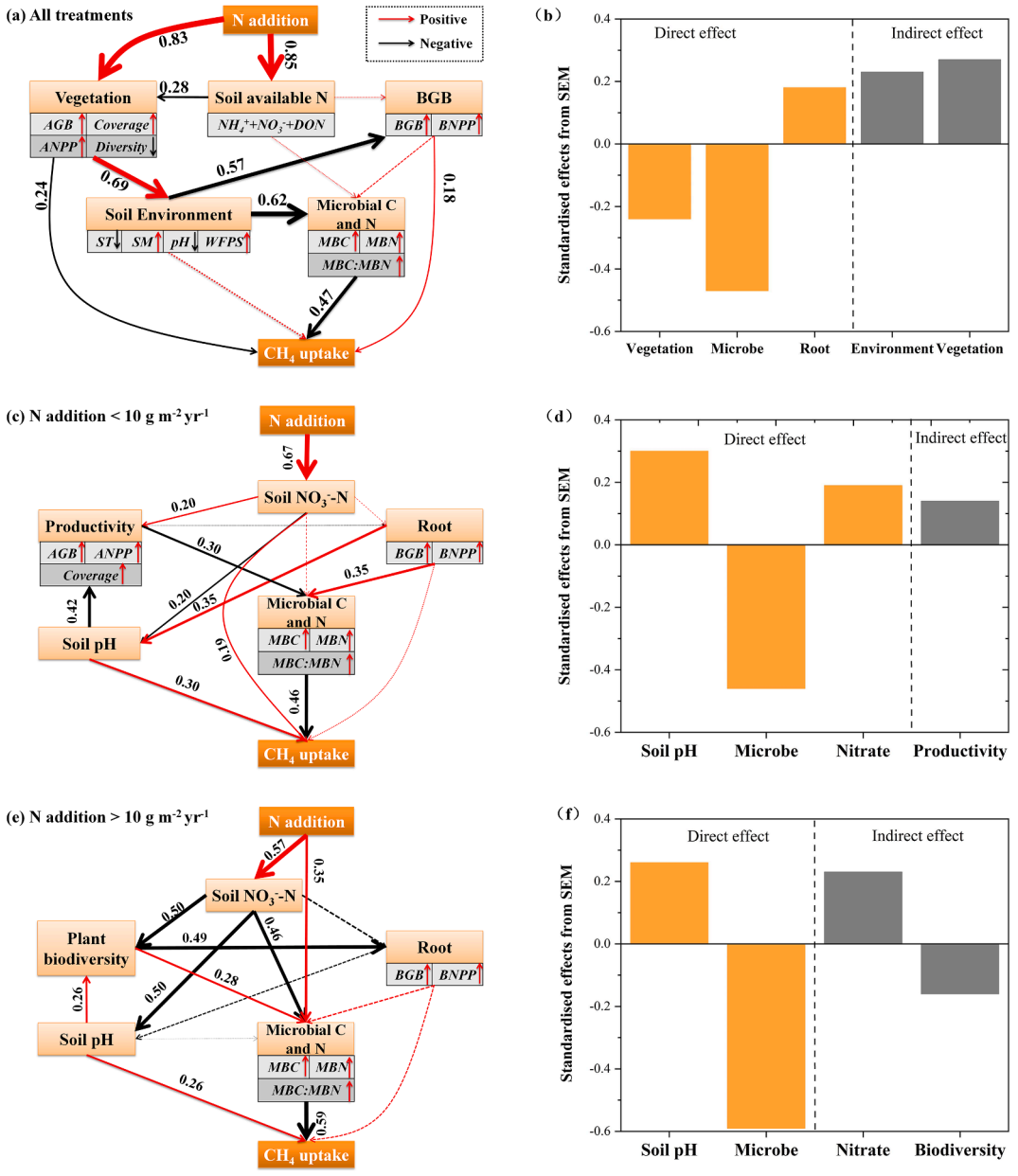

Fig. 5. Direct and indirect effects of vegetation characteristics, root dynamic, soil pH and microorganisms on CH_4 uptake under all treatments (a) (n = 144, R^2 = 0.21, χ^2 = 1.28, *df* = 8, *P* = 0.99, RMSEA = 0.00, AIC = 41.42, GFI = 1.00, CFI = 1.00), N addition rate of 0, 1, 2, 4 and 8 g N m^{-2} yr^{-1} (c) (n = 90, R^2 = 0.24, χ^2 = 5.12, *df* = 7, *P* = 0.64, RMSEA = 0.00, AIC = 47.18, GFI = 0.98, CFI = 1.00), and 16, 24 and 32 g N m^{-2} yr^{-1} (e) (n = 54, R^2 = 0.29, χ^2 = 4.5, *df* = 6, *P* = 0.61, RMSEA = 0.00, AIC = 48.49, GFI = 0.98, CFI = 1.00). Single-headed arrows indicate the hypothesized direction of causation. Red and black solid arrows indicate positive and negative relationships, respectively. Dash arrows indicate insignificant relationship. The arrow width is proportional to the strength of the relationship. Multiple-layer rectangles represent the first component from the PC analysis (Table S3). Standardized direct and indirect effects of biotic and abiotic factors on CH_4 uptake under N addition rate from 0 ~ 32 g m^{-2} yr^{-1} (b), 0 ~ 8 (<10) g m^{-2} yr^{-1} (d) and from 16 ~ 32 (>10) g m^{-2} yr^{-1} (f). (For interpretation of the references to colour in this figure legend, the reader is referred to the web version of this article.)

gene abundance was 6.75 g N m^{-2} yr^{-1} (Fig. 2e). In addition, the RDA results illustrated that the *pmoA* gene abundances had a small projection on the CH_4 uptake rate arrow (Fig. 4a), which indicated that the functional gene changes could not fully explain the changes in CH_4 flux in the saline-alkaline grassland.

The soil temperature, WFPS and soil pH are important environmental factors that drive methanotrophs (Zhang et al., 2020, Kou et al., 2020). We attributed the soil exchangeable Na^+ to be a key factor in saline-alkaline soil (Fig. S1). In the present study, the *N*-induced soil acidification promoted CH_4 uptake either with low (Fig. 5d) or high (Fig. 5f) N additions. Although the soil temperature exhibited significant decreases with N enrichments (Fig. 2a), their effects on CH_4 uptake were limited, which indicated that the methanotrophs were not sensitive to small soil temperature changes (~1℃) in the temperate region. The N additions had no effects on the soil exchangeable Na^+ (Fig. S3a) or WFPS (Fig. 2b); consequently, they were not involved in the regulation of CH_4 uptake.

The rate of increase of NO_3^--N in the soil was faster than that of NH_4^+-N with increasing N addition levels (Fig. 2e, f). Although NH_4^+-N is generally considered to be the N source for methanotrophs, NO_3^--N can be used when microbes experience N starvation (Rigler and Zechmeister-Boltenstern, 1999; Schimel and Weintraub, 2003). In addition, the NO_3^--N concentration, as a potential alternative electron acceptor, was a key factor in the CH_4 oxidation process (Kolb, 2009). Therefore, increasing the NO_3^--N concentrations promoted CH_4 uptake

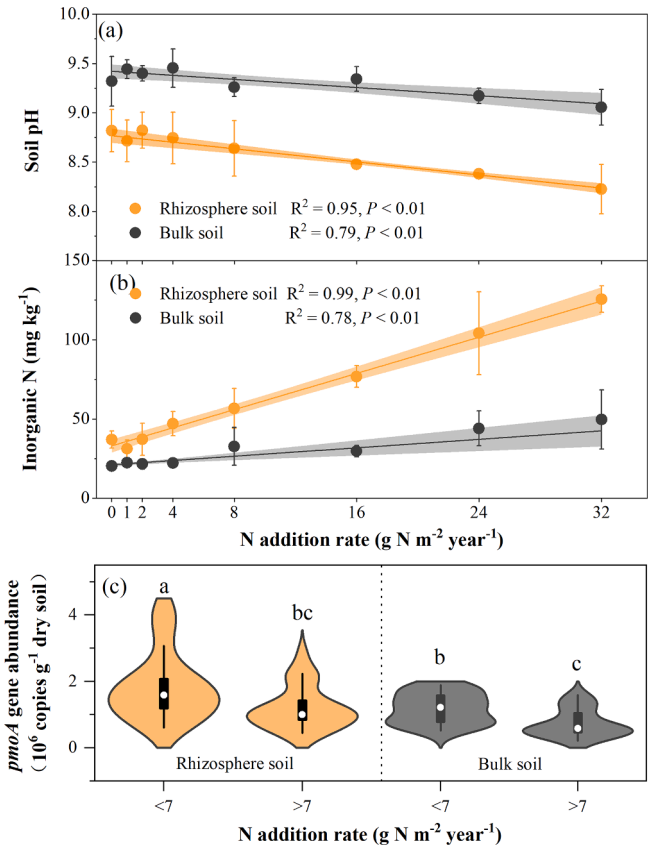

Fig. 6. Changes of soil pH (a), inorganic N concentration (b) along the N addition rate in rhizosphere and bulk soils. The *pmoA* gene abundance in rhizosphere and bulk soils under lower (<7 g m^{-2} yr^{-1}) and higher (>7 g m^{-2} yr^{-1}) N addition (c), different lowercase letters denoted significant difference between treatments ($p < 0.05$).

(Fig. 5d, f).

The MBC:MBN ratios can indicate changes in the microbial community (Paul, 2007) and N competition among microbes (Wild et al., 2017). In the present study, high N addition levels were associated with higher MBC:MBN ratios than low N addition levels (the mean of N_0, N_1, N_2, N_4 and N_8 was 6.53 and that of N_{16}, N_{24} and N_{32} was 8.02). The methanotroph community in saline-alkaline soils may change, as alkaliphilic methanotrophs belong to a specific flora (Reddy et al., 2020). Kolb (2009) reported that excessive N amounts converted methanotrophic communities to methanol-utilizing communities, so the ability of soil CH_4 oxidation decreased with high N additions. However, in the absence of changes in the microbial community, high MBC:MBN ratios increased the microbial N demand and promoted other microbes to compete for the soil available N with methanotrophs, which decreased the CH_4 uptake (Fig. 5d, f).

4.3. Regulation of methane by plant community changes

The impacts of plant community changes on the soil CH_4 uptake levels in upland ecosystems have rarely been studied. Because methanotrophs use CH_4 as both an energy and carbon source and unlike other soil microbes that are usually easily decomposable in carbon-limited soils, *N*-induced increases in plant carbon inputs may have little impact on soil CH_4 uptake. However, plants subjected to biotic and abiotic stresses (e.g., under high salinity and pH stress) can induce changes in transcriptomics and metabolomics, which result in changes of root and leaf exudates (Liu et al., 2020). These exudates, including flavonoids (Hassan and Mathesius, 2012), coumarins, triterpenes (Huang et al., 2019) and aromatic compounds (Schulz-Bohm et al., 2018), affect the microbiome. The changes in plant exudates altered the plant-associated microbial community (Gu et al., 2020) and, most likely, the methanotrophs.

The structural equation model analysis showed that the pathway of either high (Fig. 5c) or low (Fig.5e) N-induced changes in plant biomass or diversity affected soil temperature and moisture (physical pathways). The pathway did not affect the methane oxidation process, as was hypothesized (Fig. 1). These responses indicated that the rhizospheric effect (chemical pathway) is the main pathway of N-input-plant-methanotrophs interaction.

As the soil pH decreased with increasing NO_3^--N concentrations, which is the main N source for plants in soils lacking NH_4^+-N (Chen et al., 2021), the *N*-induced increase in NO_3^--N promoted plant productivity. This can increase the quantities of substrates that are easily decomposed by microorganisms (Pichon et al., 2020) and can alleviate the soil available N competition between other microorganisms and methanotrophs. Therefore, the increased productivity indirectly promoted CH_4 uptake (the standard effect from SEM was 0.14, $p < 0.05$) by influencing the microbial community with low N addition levels (<10.12 g N m^{-2} yr^{-1}). With high N addition levels (>10.12 g N m^{-2} yr^{-1}), the plant biodiversity (Shannon–Wiener index) decreased (Fig. 2h), which resulted in nitrophillous plants (e.g., Gramineae) dominating the plant community (Chen et al., 2021), which is detrimental to the microbial community (Zak et al., 2003), including methanotrophs, due to the N competition among plants and microbes and the simplification of root exudates. Consequently, the decreased plant biodiversity had an indirect negative effect on CH_4 uptake. Another possible scenario is that the plant biodiversity mediates the chemistry of plant litter and root exudates, which promotes the activities of microorganisms (Hassan et al., 2019).

Another possible mechanism was that the rhizosphere was the hot spot for plant–microbe interactions, in which the impact on methanotrophs was mediated by allelopathic effects and acidification of root exudates (Carvalhais et al., 2015, Lombardi et al., 2018, Wang et al., 2016). In this current study, the big differences of soil pH, inorganic N concentration and *pmoA* gene abundance between rhizosphere and the bulk soils was found (Fig. 6) and should be crucial for CH_4 oxidation process. Therefore, the root dynamics had a significant effect on CH_4 uptake (standard effect from SEM was 0.18, $p < 0.05$) when all treatments were considered in the SEM analysis. The RDA also confirmed that the root productivity positively affected CH_4 uptake (Fig. 4a). However, the response pattern of plant rhizosphere exudates with increasing N additions is not yet clear, and which exudates impact methanotrophs is also unknown. In-depth research on root exudates-methanotroph interactions is required in the future.

5. Conclusions

The saline-alkaline grassland was a weak CH_4 sink. A unimodal pattern of CH_4 uptake in response to increased N addition gradients was found, with the N threshold triggering a peak at ~10 g m^{-2} yr^{-1}. The nitrogen addition-induced changes in plant productivity and diversity indirectly affected the CH_4 uptake at low and high N levels, respectively. The plants regulated (interpretation rate is 14 %–21 %) soil CH_4 oxidation in response to increasing N addition levels in a saline-alkaline grassland probably attributed to the rhizosphere action on methanotrophs due to the *N*-induced changes in root activity. Our results indicate that studies on the underlying mechanisms of how the rhizospheric effects regulate methanotroph activity are needed in saline-alkaline grasslands.

Declaration of Competing Interest

The authors declare that they have no known competing financial interests or personal relationships that could have appeared to influence the work reported in this paper.

Data availability

Data will be made available on request.

Acknowledgements

We thank Jie Hao, Hui Zheng, Jiamin Qin, Jianhua Gui, Xiaoyuan Wei, Xuedong Yan, Zuoen Zhang, Hengyu Wang, Xiaojie Zhao for their field and laboratory measurement. This research was supported financially by the National Natural Science Foundation of China (31800402, 31872406); High Level Talents Project of Shanxi Agricultural University (2021XG008); Shanxi Key Laboratory Project (202104010910017); Science and technology innovation project of colleges and universities in Shanxi Province (2020L0144); Key Laboratory of Vegetation Ecology, Ministry of Education; and Science and Technology Innovation Fund of Shanxi Agricultural University (2018YJ34).

Appendix A. Supplementary data

Supplementary data to this article can be found online at https://doi.org/10.1016/j.geoderma.2022.116235.

References

Aalto, J., Roux, P., Luoto, M., 2013. Vegetation mediates soil temperature and moisture in Arctic-alpine environments. Arct. Antarct. Alp. Res. 45 (4), 429–439. https://doi.org/10.1657/1938-4246-45.4.429.

Aronson, E.L., Helliker, B.R., 2010. Methane flux in non-wetland soils in response to nitrogen fertilization: a meta-analysis. Ecology 91, 3242–3251. https://doi.org/10.1890/09-2185.1.

Barillot, C.D.C., Sarde, C.O., Bert, V., Tarnaud, E., Cochet, N., 2013. A standardized method for the sampling of rhizosphere and rhizoplan soil bacteria associated to a herbaceous root system. Annals of Microbiology 63, 471–476. https://doi.org/10.1007/s13213-012-0491-y.

Bhardwaj, Y., Dubey, S., 2020. Changes in pmoA gene containing methanotrophic population and methane oxidation potential of dry deciduous tropical forest soils. Curr. Sci. 118 (5), 750–758. https://doi.org/10.18520/cs/v118/i5/750-758.

Bodelier, P.L.E., Laanbroek, H.J., 2004. Nitrogen as a regulatory factor of methane oxidation in soils and sediments. FEMS Microbiol. Ecol. 47, 265–277. https://doi.org/10.1016/S0168-6496(03)00304-0.

Bolker, B.M., Brooks, M.E., Clark, C.J., Geange, S.W., Poulsen, J.R., Stevens, M.H.H., White, J.S.S., 2009. Generalized linear mixed models: a practical guide for ecology and evolution. Trends Ecol. Evol. 24 (3) https://doi.org/10.1016/j.tree.2008.10.008.

Bürgmann, H., 2011. Methane oxidation (aerobic). In: Reitner, J., Thiel, V. (Eds.), Encyclopedia of Geobiology. Encyclopedia of Earth Sciences Series. Springer, Dordrecht. https://doi.org/10.1007/978-1-4020-9212-1_139.

Burckhardt C., B., Kroll, B., Frömter, E., 1992. Proton transport mechanism in the cell membrane of Xenopus laevis oocytes. Pflügers Archiv European Journal of Physiology. https://doi.org/10.1007/BF00378644.

Carvalhais, L.C., Dennis, P.G., Badri, D.V., Kidd, B.N., Vivanco, J., Schenk, P., 2015. Linking jasmonic acid signaling, root exudates, and rhizosphere microbiomes. Molecular Plant−Microbe. Interaction 28, 1049–1058. https://doi.org/10.1094/MPMI-01-15-0016-R.

Chang, R.Y., Liu, X.Y., Wang, T., Li, N., Bing, H.J., 2021. Stimulated or inhibited response of methane flux to nitrogen addition depends on nitrogen levels. J. Geophys. Res. Biogeosci. 126 (11), 1–10. https://doi.org/10.1029/2021JG006600.

Chen, Y., Bonkowski, M., Shen, Y., Griffiths, B.S., Jiang, Y., Wang, X., Sun, B., 2020b. Root ethylene mediates rhizosphere microbial community reconstruction when chemically detecting cyanide produced by neighboring plants. Microbiome 8 (4), 1–17. https://doi.org/10.1186/s40168-019-0775-6.

Chen, S., Hao, T.X., Goulding, K., Misselbrook, T., Liu, X.J., 2019. Impact of 13-years of nitrogen addition on nitrous oxide and methane fluxes and ecosystem respiration in a temperate grassland. Environ. Pollut. 252, 675–681. https://doi.org/10.1016/j.envpol.2019.03.069.

Chen, S.H., Lin, Q.S., Xiao, Y., Deng, Y.Y., Chang, C.Q., Zhong, G.H., Hu, M.Y., Zhang, L. H., Permyakov, E.A., 2013. Monooxygenase, a novel beta-cypermethrin degrading enzyme from streptomyces sp. PLoS ONE 8 (9), e75450.

Chen, X.P., Wang, G.X., Zhang, T., Mao, T.X., Wei, D., Hu, Z.Y., Song, C.L., 2017. Effects of warming and nitrogen fertilization on GHG flux in the permafrost region of an alpine meadow. Atmos. Environ. 157 (5), 111–124. https://doi.org/10.1016/j.atmosenv.2017.03.024.

Chen, X.P., Wang, Y.H., Li, J.Y., Li, R., Zhao, X., Dong, K.H., 2020a. Analysis of soil salinity and phosphorous availability of grassland under different saline spot coverage. Journal of Shanxi. Agric. Sci. 48 (9), 1481–1486. https://doi.org/10.3969/j.issn.1002-2481.2020.09.25 in Chinese.

Chen, X.P., Zhang, T., Guo, R.Y., Li, H.Y., Zhang, R., Degen, A.A., Huang, K.W., Wang, X. M., Bai, Y.F., Shang, Z.H., 2021. Fencing enclosure alters nitrogen distribution patterns and tradeoff strategies in an alpine meadow on the Qinghai-Tibetan Plateau. Catena 197, 104948. https://doi.org/10.1016/j.catena.2020.104948.

Deng, Y.C., Liu, Y.Q., Dumont, M., Conrad, R., 2017. Salinity affects the composition of the aerobic methanotroph community in alkaline lake sediments from the Tibetan Plateau. Microb. Ecol. 73, 101–110. https://doi.org/10.1007/s00248-016-0879-5.

Farrell, M., Prendergast-Miller, M., Jones, D.L., Hill, P.W., Condron, L.M., 2014. Soil microbial organic nitrogen uptake is regulated by carbon availability. Soil Biol. Biochem. 77, 261–267.

Gao, Y.Z., Giese, M., Lin, S., Sattelmacher, B., Zhao, Y., Brueck, H., 2008. Belowground net primary productivity and biomass allocation of a grassland in Inner Mongolia is affected by grazing intensity. Plant Soil 307, 41–50. https://doi.org/10.1007/s11104-008-9579-3.

Gu, Y., Wang, X., Yang, T., Friman, V.-P., Geisen, S., Wei, Z., Xu, Y., Jousset, A., Shen, Q., Morriën, E., 2020. Chemical structure predicts the effect of plant-derived low-molecular weight compounds on soil microbiome structure and pathogen suppression. Funct. Ecol. 34 (10), 2158–2169.

Hassan, S., Mathesius, U., 2012. The role of flavonoids in root-rhizosphere signaling: opportunities and challenges for improving plant–microbe interactions. J. Exp. Bot. 63, 3429–3444. https://doi.org/10.1093/jxb/err430.

Hassan, M.K., McInroy, J.A., Kloepper, J.W., 2019. The interactions of rhizodeposits with plant growth-promoting rhizobacteria in the rhizosphere: a review. Agriculture 9, 142. https://doi.org/10.3390/agriculture9070142.

Hassani, A., Azapagic, A., Shokri, N., 2020. Predicting long-term dynamics of soil salinity and sodicity on a global scale. PNAS 117 (52), 33017–33027.

Hedges, L.V., Gurevitch, J., Curtis, P.S., 1999. The meta-analysis of response ratios in experimental ecology. Ecology 80, 1150–1156. https://doi.org/10.2307/177062.

Hooper, D., Coughlan, J., Mullen, M., 2008. Structural equation modelling: guidelines for determining model fit. Electr. J. Bus. Res. Methods 6, 53–60. https://doi.org/10.3109/03005364000000039.

Hu, L.F., Robert, C.A.M., Cadot, S., Zhang, X., Ye, M., Li, B.B., Manzo, D., Chervet, N., Steinger, T., van der Heijden, M.G.A., Schlaeppi, K., Erb, M., 2018. Root exudate metabolites drive plant-soil feedbacks on growth and defense by shaping the rhizosphere microbiota. Nat. Commun. 9 (1), 2738. https://doi.org/10.1038/s41467-018-05122-7.

Huang, X.F., Chaparro, J.M., Reardon, R.F., Zhang, R.F., Shen, Q.R., Vivanco, J.M., 2014. Rhizosphere interactions: root exudates, microbes, and microbial communities. Botany 92, 267–275. https://doi.org/10.1139/cjb-2013-0225.

Huang, A.C., Jiang, T., Liu, Y.X., Bai, Y.C., Reed, J., Qu, B.Y., Goossens, A., Nützmann, H. W., Bai, Y., Osbourn, A., 2019. A specialized metabolic network selectively modulates Arabidopsis root microbiota. Science 364, eaau6389. https://doi.org/10.1126/science.aau6389.

Kimmel, K., Furey, G.N., Hobbie, S.E., Isbell, F., Tilman, D., Reich, P.B., 2020. Diversity-dependent soil acidification under nitrogen enrichment constrains biomass productivity. Glob. Change Biol. 26 (11), 6594–6603. https://doi.org/10.1111/gcb.15329.

Kolb, S., 2009. Aerobic methanol-oxidizing Bacteria in soil. FEMS Microbiol. Lett. 300, 1–10. https://doi.org/10.1111/j.1574-6968.2009.01681.x.

Kolb, S., Knief, C., Stubner, S., Conrad, R., 2003. Quantitative detection of methanotrophs in soil by novel pmoA-targeted real-time PCR assays. Appl. Environ. Microbiol. 69, 2423–2429. https://doi.org/10.1128/AEM.69.5.2423-2429.2003.

Kou, Y.P., Zhao, W.Q., Liu, Y.J., Wu, Y.H., Xiao, J.T., Wang, X.H., Bing, H.J., Liu, Q., 2021. Diversity patterns and drivers of methanotrophic gene distribution in forest soil across a large latitudinal gradient. Global Ecol. Biogeogr. 30 (10), 2004-2015. https://doi.org/ 10.1111/geb.13362.

Lafuente, A., Bowker, M.A., Delgado-Baquerizo, M., Durán, J., Singh, B.K., Maestre, F.T., 2019. Global drivers of methane oxidation and denitrifying gene distribution in dryland. Glob. Ecol. Biogeogr. 9, 1230–1243. https://doi.org/10.1111/geb.12928.

Li, X.Y., Cheng, S.L., Fang, H.J., Yu, G.R., Dang, X.S., Xu, M.J., Wang, L., Si, G.Y., Geng, J., He, S., 2015. The contrasting effects of deposited NH_4^+ and NO_3^- on soil CO_2, CH_4 and N_2O fluxes in a subtropical plantation, southern China. Ecol. Eng. 85, 317–327. https://doi.org/10.1016/j.ecoleng.2015.10.003.

Li, X.L., He, H., Yuan, W.P., Li, L.H., Xu, W.F., Liu, W., Shi, H.Q., Hou, L.Y., Chen, J.Q., Wang, Z.P., 2018. Response of soil methane uptake to simulated nitrogen deposition and grazing management across three types of steppe in Inner Mongolia, China. Sci. Total Environ. 612, 799–808. https://doi.org/10.1016/j.scitotenv.2017.08.236.

Liu, H.W., Brettell, L.E., Qiu, Z.G., Singh, B.K., 2020. Microbiome-mediated stress resistance in plants. Trends Plant Sci. 25 (8), 733–743. https://doi.org/10.1016/j.tplants.2020.03.014.

Lombardi, N., Vitale, S., Turrà, D., Reverberi, M., Fanelli, C., Vinale, F., Marra, R., Ruocco, M., Pascale, A., d'Errico, G., Woo, S.L., Lorito, M., 2018. Root exudates of stressed plants stimulate and attract Trichoderma soil fungi. Mol. Plant-Microbe Interact. 31, 982–994. https://doi.org/10.1094/MPMI-12-17-0310-R.

Ma, L., Yang, H.L., Pan, Z.L., Rong, Y.P., 2020. In situ measurements and meta−analysis reveal that land-use changes combined with low nitrogen application promote methane uptake by temperate grasslands in China. Sci. Total Environ. 706, 136048 https://doi.org/10.1016/j.scitotenv.2019.136048.

Marschner, H., 1995. Mineral Nutrition of Higher Plants. Academic Press, London.

Moreau, D., Bardgett, R.D., Finlay, R.D., Jones, D.L., Philippot, L., Power, S., 2019. A plant perspective on nitrogen cycling in the rhizosphere. Funct. Ecol. 33 (4), 540–552.

Pathak, H., Rao, D.L.N., 1998. Carbon and nitrogen mineralization from added organic matter in saline and alkali soils. Soil Biol. Biochem. 30 (6), 695–702. https://doi.org/10.1016/S0038-0717(97)00208-3.

Paul, E.A., 2007. Soil Microbiology, Ecology, and Biochemistry. 3rd Edition (Academic Press, Amsterdam). https://doi.org/10.2136/sssaj2007.0017br.

Peng, Y.F., Wang, G.Q., Li, F., Yang, G.B., Fang, K., Liu, L., Qin, S.Q., Zhang, D.Y., Zhou, G.Y., Fang, H.J., Liu, X.J., Liu, C.Y., Yang, Y.H., 2019. A unimodal response of soil methane consumption to increasing nitrogen additions. Environ. Sci. Technol. 53 (8), 4150–4160. https://doi.org/10.1021/acs.est.8b04561.

Pichon, N.A., Cappelli, S.L., Soliveres, S., Hölzel, N., Klaus, V.H., Kleinebecker, T., Allan, E., Stevens, C., 2020. Decomposition disentangled: a test of the multiple mechanisms by which nitrogen enrichment alters litter decomposition. Funct. Ecol. 34 (7), 1485–1496.

Reddy R., K., Rai K., R., Green J., S., Chetri K., J., 2020. Effect of pH on methane oxidation and community composition in landfill cover soil. Journal of Environmental Engineering 146 (6), 04020037. https://doi.org/10.1061/(asce)ee.1943-7870.0001712.

Rigler, E., Zechmeister-Boltenstern, S., 1999. Oxidation of ethylene and methane in forest soils-effect of CO_2 and mineral nitrogen. Geoderma 90, 147–159. https://doi.org/10.1016/S0016-7061(98)00099-8.

Schimel, J.P., Weintraub, M.N., 2003. The implications of exoenzyme activity on microbial carbon and nitrogen limitation in soil: a theoretical model. Soil Biol. Biochem. 35, 549–563. https://doi.org/10.1016/S0038-0717(03)00015-4.

Schulz-Bohm, K., Gerards, S., Hundscheid, M., Melenhorst, J., de Boer, W., Garbeva, P., 2018. Calling from distance: attraction of soil bacteria by plant root volatiles. ISME J. 12, 1252–1262. https://doi.org/10.1038/s41396-017-0035-3.

Setia, R., Marschner, P., Baldock, J., Chittleborough, D., Verma, V., 2011. Relationships between carbon dioxide emission and soil properties in salt-affected landscapes. Soil Biol. Biochem. 43 (3), 667–674. https://doi.org/10.1016/j.soilbio.2010.12.004.

Spellerberg, I.F., 2008. Encyclopedia of Ecology. Shannon−Wiener Index, pp. 3249–3252.

Täumer, J., Kolb, S., Boeddinghaus, R.S., Wang, H., Schöning, I., Schrumpf, M., Urich, T., Marhan, S., 2020. Divergent drivers of the microbial methane sink in temperate forest and grassland soils. Glob. Change Biol. 27 (4), 929–940. https://doi.org/10.1111/gcb.15430.

Tian, H., Lu, C., Ciais, P., Michalak, A.M., Canadell, J.G., Saikawa, E., Huntzinger, D.N., Gurney, K.R., Sitch, S., Zhang, B., Yang, J., Bousquet, P., Bruhwiler, L., Chen, G., Dlugokencky, E., Friedlingstein, P., Melillo, J., Pan, S., Poulter, B., Prinn, R., Saunois, M., Schwalm, C.R., Wofsy, S.C., 2016. The terrestrial biosphere as a net source of greenhouse gases to the atmosphere. Nature 531, 225–228. https://doi.org/10.1038/nature16946.

Tian, D.S., Niu, S.L., 2015. A global analysis of soil acidification caused by nitrogen addition. Environ. Res. Lett. 10 (2), 024019 https://doi.org/10.1088/1748-9326/10/2/024019.

Trivedi, P., Leach, J.E., Tringe, S.G., Sa, T.M., Singh, B.K., 2020. Plant-microbiome interactions: from community assembly to plant health. Nat. Rev. Microbiol. 18, 607–621. https://doi.org/10.1038/s41579-020-0412-1.

Unteregelsbacher, S., Gasche, R., Lipp, L., Sun, W., Kreyling, O., Geitlinger, H., Kögel-Knabner, I., Papen, H., Kiese, R., Schmid, H.-P., Dannenmann, M., 2013. Increased methane uptake but unchanged nitrous oxide flux in montane grasslands under simulated climate change conditions. Eur. J. Soil Sci. 64 (5), 586–596.

Wang, X.J., Tang, C.X., Severi, J., Butterly, C.R., Baldock, J.A., 2016. Rhizosphere priming effect on soil organic carbon decomposition under plant species differing in soil acidification and root exudation. New Phytol. 3, 864–873. https://doi.org/10.1111/nph.13966.

Wang, C.H., Zhu, F., Zhao, X., Dong, K.H., 2014. The effects of N and P additions on microbial N transformations and biomass on saline-alkaline grassland of Loess Plateau of Northern China. Geoderma 213, 419–425. https://doi.org/10.1016/j.geoderma.2013.08.003.

Wei, D., Xu, R., Tenzin, T., Wang, Y.S., Wang, Y.H., 2014. Considerable methane uptake by alpine grasslands despite the cold climate: In situ measurements on the central Tibetan Plateau, 2008–2013. Glob. Change Biol. 21, 777–788. https://doi.org/10.1111/gcb.12690.

Wei, D., Xu, R., Tenzin, T., Dai, D.X., Wang, Y.S., Wang, Y.H., 2015. Revisiting the role of CH_4 emissions from alpine wetlands on the Tibetan Plateau: evidence from two in situ measurements at 4758 to 4320 m above sea level. J. Geophys. Res. 120, 1741–1750. https://doi.org/10.1002/2015JG002974.

Wild, B., Alaei, S., Bengtson, P., Bodé, S., Boeckx, P., Schnecker, J., Mayerhofer, W., Rütting, T., 2017. Short-term carbon input increases microbial nitrogen demand, but not microbial nitrogen mining, in a set of boreal forest soils. Biogeochemistry 136 (3), 261–278. https://doi.org/10.1007/s10533-017-0391-0.

Willams, A., de Vries, F.T., 2019. Plant root exudation under drought: implications for ecosystem functioning. New Phytol. 225 (5), 1899–1905. https://doi.org/10.1111/nph.16223.

Yan, N., Marschner, P., 2013. Microbial activity and biomass recover rapidly after leaching of saline soils. Biol. Fertil. Soils 49, 367–371. https://doi.org/10.1007/s00374-012-0733-y.

Yue, P., Cui, X.Q., Wu, W.C., Gong, Y.M., Li, K.H., Goulding, K., Liu, X.J., 2019. Impacts of precipitation, warming and nitrogen deposition on methane uptake in a temperate desert. Biogeochemistry 146 (1), 17–29. https://doi.org/10.1007/s10533-019-00606-0.

Zak, D.R., Holmes, W.E., White, D.C., Peacock, A.D., Tilman, D., 2003. Plant diversity, soil microbial community, and ecosystem function: are there any links? Ecology 84 (8), 2042–2050. https://doi.org/10.1890/02-0433.

Zhalnina, K., Louie, K., Hao, Z., Mansoori, N., Rocha, U., Shi, S., Cho, H., Karaoz, U., Loqué, D., Bowen, B., Firestone, M., Northern, T., Brodie, E., 2018. Dynamic root exudate chemistry and microbial substrate preferences drive patterns in rhizosphere microbial community assembly. Nat. Microbiol. 3 (4), 470–480. https://doi.org/10.1038/s41564-018-0129-3.

Zhang, L.Y., Adams, J.M., Dumont, M.G., Li, Y.T., Shi, Y., He, D., He, J.S., Chu, H.Y., 2019. Distinct methanotrophic communities exist in habitats with different soil water contents. Soil Biol. Biochem. 132 (1), 143–152. https://doi.org/10.1016/j.soilbio.2019.02.007.

Zhang, L.Y., Dumont, M.G., Bodelier, P.L.E., Adams, J.M., He, D., Chu, H.Y., 2020. DNA stable-isotope probing highlights the effects of temperature on functionally active methanotrophs in natural wetlands. Soil Biol. Biochem. 149, 107954 https://doi.org/10.1016/j.soilbio.2020.107954.

Zhang, W., Liu, C.Y., Zheng, X.H., Fu, Y.F., Hu, X.X., Cao, G.M., Butterbach-Bahl, K., 2014. The increasing distribution area of zokor mounds weaken greenhouse gas uptakes by alpine meadows in the Qinghai-Tibetan Plateau. Soil Biol. Biochem. 71, 105–112. https://doi.org/10.1016/j.soilbio.2014.01.005.